Appendix 1

A Standard System of Characterization for Olefin Metathesis Catalysts

This chapter was taken in part from:

Ritter, T.; Hejl, A.; Wenzel, A. G.; Funk, T. W.; Grubbs, R. H. *Organometallics* **2006**, *25*, 5740–5745.

A Standard System of Characterization for Olefin Metathesis Catalysts

Introduction

In the past decade, the development of well-defined catalysts has established olefin metathesis as a useful synthetic tool in both organic and polymer chemistry.[1] Here, we identify a series of transformations to serve as a useful, general, and easily applicable platform for catalyst comparison. Such a standard methodology is of vital importance in properly assessing the impact of changes made in a catalyst framework and should work hand in hand with rational catalyst design. We do not intend to provide a comprehensive series of reactions or to identify an ideal catalyst for every transformation. Instead, the idea is to offer a concise method for the comparison of ruthenium-based olefin metathesis catalysts under specific reaction conditions to have a valuable, meaningful tool for the development of new catalysts.

A standard set of reactions was established to obtain a maximum amount of qualitative and quantitative data with minimal synthetic effort. To cover a wide range of reactivity and functionality with our assay, we have selected three distinctly different reaction types: ring-closing metathesis (RCM), cross metathesis (CM), and ring-opening metathesis polymerization (ROMP). Particularly challenging reactions have been included in the reaction panel to identify unsolved problems in olefin metathesis where the development of new, more active catalysts is needed. For the sake of simplicity, the selected substrates are either commercially available or prepared in a single synthetic step. The progression of the reactions over time is studied, which allows for the quantification of results and the acquisition of rate data where appropriate. The base set of standard reactions we have chosen is not meant to be exhaustive but could be extended to test catalysts with specific applications, such as catalyst activity at low temperature[2] or in water.[3]

Throughout this article, catalyst performance will be described with respect to efficiency and its components: selectivity, activity, and stability (Figure A1.1). The efficiency of a catalyst can be determined by measuring the yield of a desired reaction product within a given time. Efficiency can therefore be easily monitored. Selectivity can be divided into chemo- and stereoselectivity. In particular, chemoselectivity includes the ability of a catalyst to react with

certain types of olefins. The inability of a catalyst to react with a particular olefin class (e.g., tetrasubstituted double bonds) would render it inefficient for this reaction due to its chemoselectivity. Activity is a reaction-dependent, quantitative measurement and represents the reaction rate observed with a given catalyst. We define stability as the lifetime of a catalytic species during the course of a reaction; this can be monitored by the loss of activity. Hence, a catalyst must demonstrate not only activity but also sufficient stability to be efficient. An important result of this study is the observation that a given catalyst can be very efficient in one type of metathesis reaction and completely inefficient in another.

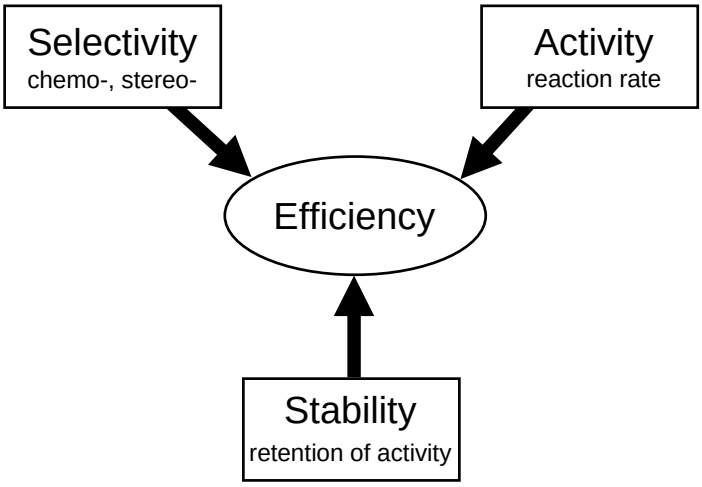

Figure A1.1. Parameters influencing catalyst efficiency.

Catalysts

The selection of ruthenium catalysts studied is given in Chart A1.1. The presented complexes **A1.1–A1.7** are among the most commonly used ruthenium catalysts for olefin metathesis.[4,5] Catalysts **A1.1**[6] (**PCy_3–P**) and **A1.2**[7] (**PCy_3–O**) are members of the class of phosphine-based catalysts. In the second generation catalysts **A1.3–A1.7**, one phosphine ligand has been replaced with an *N*-heterocyclic carbene (NHC) ligand. These include the dihydroimidazole-based catalysts **A1.3**[8] (**H_2IMes–P**) and **A1.4**[9] (**H_2IMes–O**), the imidazole-based **A1.5**[10] (**IMes–P**), and the bulky diisopropylphenyl-substituted **A1.6**[11] (**H_2IDIPP–P**). In catalyst

A1.7[12] (**H_2IMes–py**) the phosphine of **A1.3** is replaced with a pair of weakly bound bromopyridine ligands.

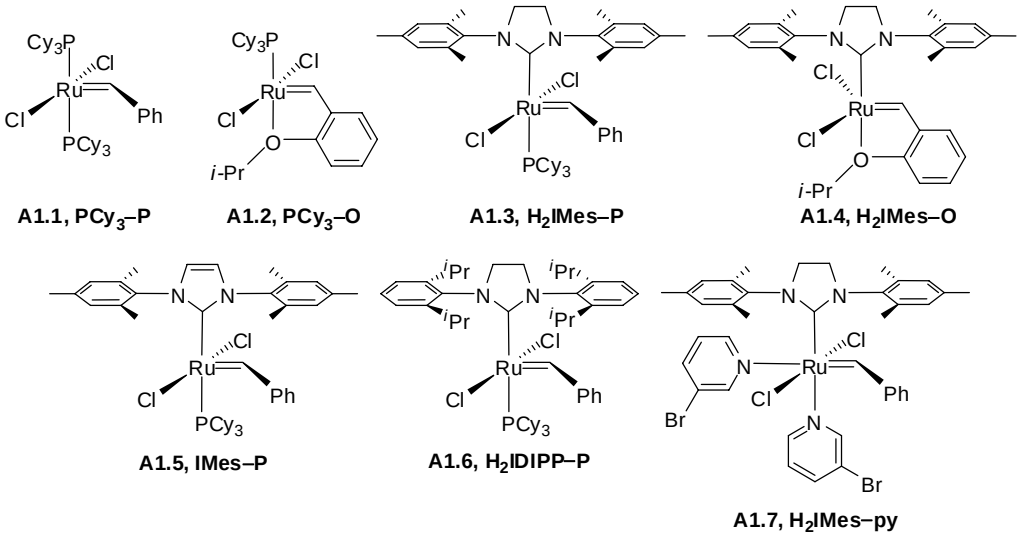

Chart A1.1. Ruthenium-Based Olefin Metathesis Catalysts Used in This Study

Ring-Closing Metathesis

RCM was the first widely used metathesis reaction in organic synthesis.[13] This reaction class was chosen as the first assay in our reaction panel due to its high degree of reproducibility, importance in synthetic chemistry, and ease to perform and monitor over time. It has been used extensively by us[14] and others[15] to test numerous catalysts; however, the multitude of different reaction conditions used has precluded direct catalyst comparisons. Three RCM reactions, the formation of di-, tri-, and tetrasubstituted double bonds, were investigated. The formation of disubstituted olefins is a good first screen of catalyst efficiency, as it is one of the easiest RCM reactions to catalyze. Tri- and tetrasubstituted olefins are more difficult to form and, hence, allow for the evaluation of catalysts with increasing efficiency. The course of the reaction is monitored by NMR spectroscopy and measures the conversion of starting material to product over time. It is important to note that, although all reactions are carried out in closed systems, results differ if the reactions are carried out in open vessels, presumably due to the formation of ethylene. However, the closed system used in this screening is valid for evaluating general differences between

catalysts. The reaction results are reproducible and have been verified in at least two independent experiments.

RCM to Form Disubstituted Olefins

The first test of catalyst efficiency is the RCM of diethyldiallyl malonate (**A1.8**) (eq A1.1). Under the given reaction conditions **A1.1–A1.7** were all found to be capable of catalyzing this reaction to complete conversion; therefore, all catalysts screened demonstrated eficiency in this reaction. The reaction progress with catalysts **A1.1–A1.4** is shown in Figure A1.2, while Figure A1.3 shows the progression of the RCM reaction catalyzed by **A1.5–A1.7**, keeping **A1.3** as a standard for comparison. Figure A1.2 illustrates that the catalysts **H_2IMes–P** and **H_2IMes–O** show similar activity, whereas **PCy_3–P** and **PCy_3–O** behave very differently. This difference is puzzling, as the structural difference (replacement of a phosphine with a chelating ether group) between the two pairs of catalysts is the same. The shape of the curves in Figures A1.2 and A1.3 may reveal important information concerning the mechanism of this reaction. To this effect, the line shape of **PCy_3–P** in Figure A1.2 is especially worth mentioning. After an initial period of high activity the reaction rate slows dramatically and continues with a much lower rate until completion of the reaction after 24 h. Although this catalyst has been known for over a decade, this intriguing feature had not yet been identified, but can be observed and quantified with this assay. The implications of this previously unobserved behavior are currently under investigation. The line shape corresponding to **PCy_3–O** is significantly different, showing an initial induction period consistent with slower catalyst initiation. Figure A1.3 illustrates the conversion profiles of second generation catalysts for the RCM of **A1.8** and reveals that the saturated **H_2IMes–P** is more active than the unsaturated **IMes–P**. **H_2IDIPP–P** is extremely active for this reaction, likely due to a combination of fast initiation and fast propagation.[16] The fast initiator **H_2IMes–py** exhibits high initial activity, but this activity decreases during the course of the reaction, which is indicative of catalyst decomposition. The relative stability of catalysts can be nicely illustrated by plotting ln([starting material]) versus time (Figure A1.4). For example, a plot of the **H_2IMes–P** data is linear, indicating pseudo-first-order rate kinetics over the course of the reaction, whereas the curvature in the logarithmic plot for the **H_2IMes–py** catalyst is consistent with catalyst

decomposition. This reduced stability of **H_2IMes–py** prevents high efficiency despite the very high activity. Additional rate analysis and rate constants for the catalysts can be found in the Experimental section.

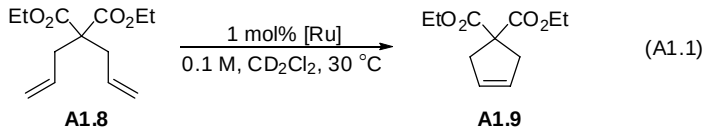

A1.8 **A1.9**

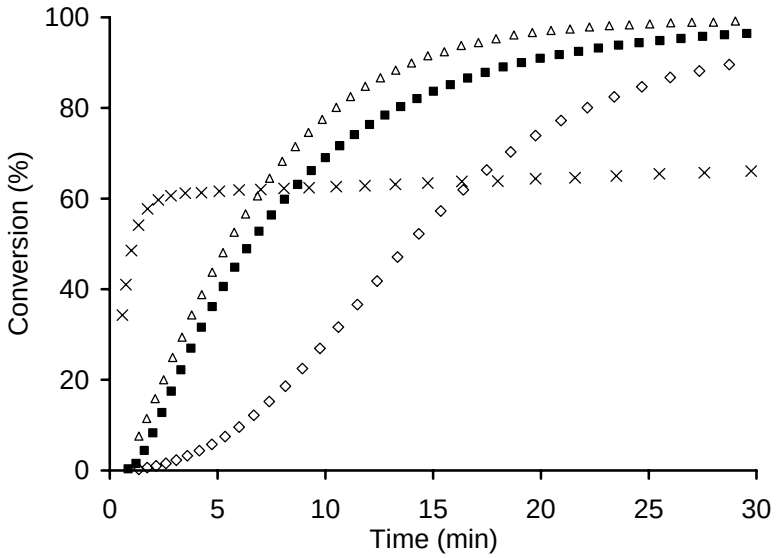

Figure A1.2. Conversion to disubstituted olefin product **A1.9** using **PCy_3–P**(×), **PCy_3–O**(◇), **H_2IMes–P**(■), and **H_2IMes–O**(△).

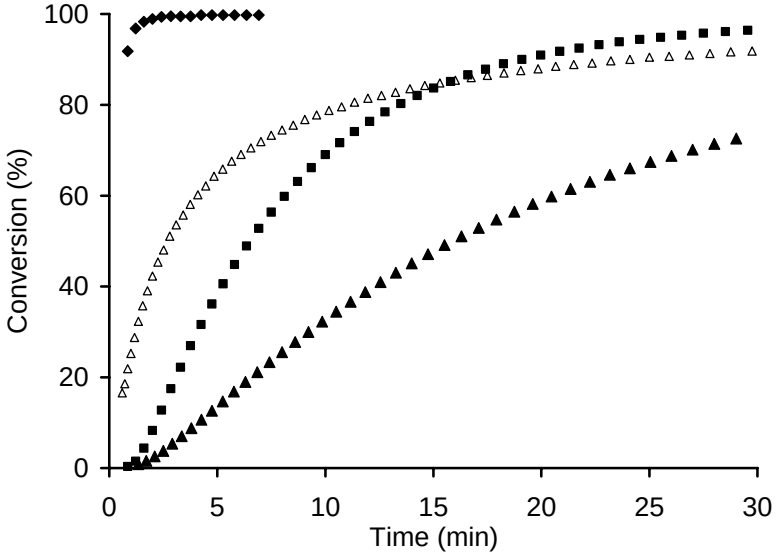

Figure A1.3. Conversion to disubstituted olefin product **A1.9** using **H_2IMes–P**(■), **IMes–P**(▲), **H_2IDIPP–P**(◆), and **H_2IMes–py**(△).

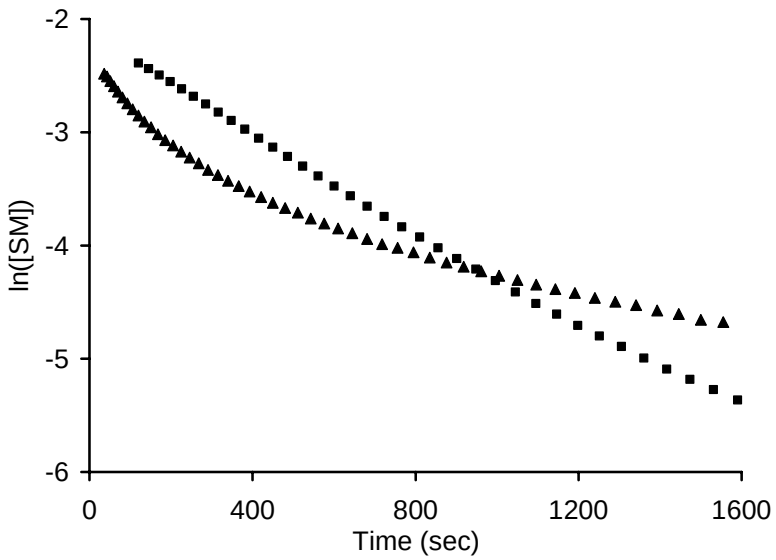

Figure A1.4. Log plots for **H_2IMes–P**(■) (linear, pseudo-first-order) and **H_2IMes–py**(▲) (curved, catalyst decomposition) as representative examples.

RCM to Form Trisubstituted Olefins

Replacement of one allyl substituent with a methallyl substituent affords diethylallylmethallyl malonate (**A1.10**), which upon RCM will furnish cyclopentene **A1.11**, featuring a trisubstituted double bond (eq A1.2). Due to steric effects, this reaction is more demanding than the corresponding RCM to form disubstituted olefin **A1.9** shown in eq A1.1 and serves as a secondary screen for complexes known to catalyze the RCM of **A1.8**. Due to the more challenging nature of this substrate, the formation of trisubstituted double bonds better highlights small differences in catalyst activity than the disubstituted case. Figure A1.5 summarizes the results for all seven catalysts examined. Here, there is a large distinction between the phosphine-based first-generation catalysts **PCy_3–P** and **PCy_3–O** and the second-generation, NHC-based catalysts. Although **PCy_3–P** and **PCy_3–O** are both capable of catalyzing the reaction to completion, the time required is significantly longer than observed with the NHC-based catalysts. This is well illustrated by comparing **IMes–P** and **PCy_3–O**. In the case of the disubstituted olefin RCM **PCy_3–O** is more active than the NHC-based **IMes–P** (Figures A1.2 and A1.3); this behavior inverts, however, in the case of trisubstituted olefins. Again, as observed in Figure A1.2, **H_2IMes–P** and **H_2IMes–O** show similar activity. The catalysts' stability can be easily

studied in this reaction due to the increased reaction times compared to the formation of disubstituted double bonds. The fast initiators **H_2IDIPP–P** and **H_2IMes–py**, for example, suffer more from catalyst instability in this challenging reaction than in the easier transformation to form disubstituted double bonds. Although initial rates are high for both catalysts, their lack of stability becomes problematic over the course of the reaction. Despite high activity, the low stability of these catalysts prevents high efficiency; **H_2IDIPP–P** and **H_2IMes–py** are the only catalysts in our study that did not catalyze the reaction shown in eq A1.2 to complete conversion.

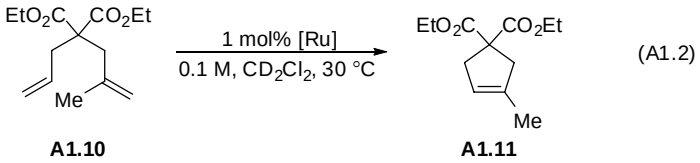

A1.10 **A1.11** (A1.2)

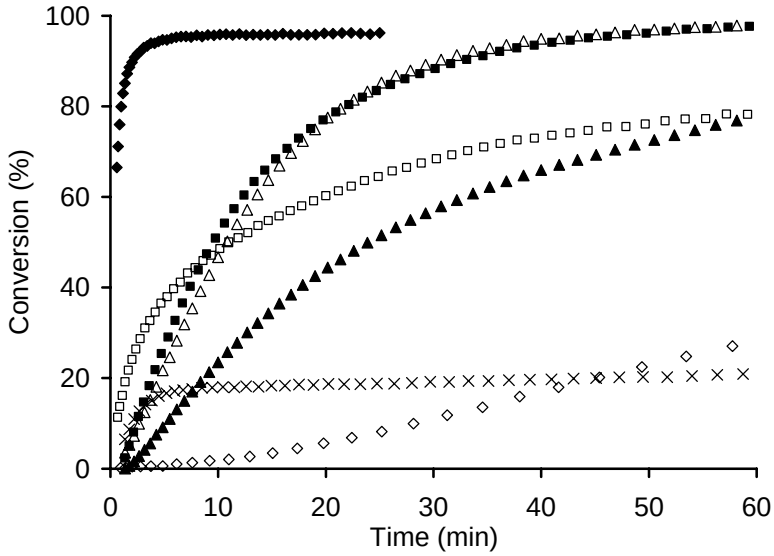

Figure A1.5. Conversion to trisubstituted olefin product **A1.11** using **PCy_3–P**(×), **PCy_3–O**(◇), **H_2IMes–P**(■), **H_2IMes–O**(△), **IMes–P**(▲), **H_2IDIPP–P**(◆), and **H_2IMes–py**(□).

RCM to Form Tetrasubstituted Olefins

This very challenging reaction (eq A1.3) typically requires high catalyst loadings and elevated reaction temperatures and can be classified as an example of a currently unsolved problem in ruthenium-catalyzed olefin metathesis. The difficulty of this reaction, however, makes it a useful addition to the set of standard reactions presented, as future, more active catalysts may be competent for this reaction. Table A1.1 lists the conversion of diethyldimethallyl malonate

(**A1.12**) to the tetrasubstituted double-bond product **A1.13** after 4 days. The first generation catalysts **PCy_3–P** and **PCy_3–O** do not catalyze this reaction under the described reaction conditions. Although very active for the RCM of **A1.8**, **H_2IMes–py** is not stable and, hence, is inefficient for this transformation. Unlike in the other two RCM reactions, **H_2IMes–P** and **H_2IMes–O** behave differently in this reaction, with **H_2IMes–P** being slightly more efficient. Although less efficient in the RCM to form di- and trisubstituted double bonds, the unsaturated NHC catalyst **IMes–P** is more efficient than **H_2IMes–P** for the generation of **A1.13**. This might be explained by the increased stability of **IMes–P** compared to its saturated counterpart. Given the long reaction times and poor yields, this reaction represents a major challenge for the design of new, more efficient catalysts in the future.

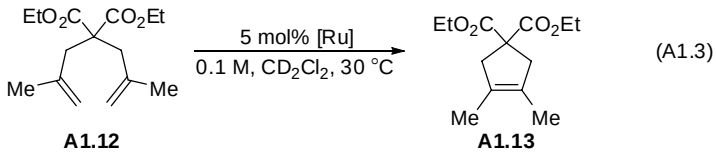

A1.12 **A1.13** (A1.3)

Table A1.1. Observed Conversions in the RCM of **A1.12** After 4 Days

Catalyst	Conversion
PCy_3–P	0 %
PCy_3–O	0 %
H_2IMes–P	17 %
H_2IMes–O	6 %
IMes–P	31 %
H_2IMes–py	0 %
H_2IDIPP–P	10 %

To summarize the RCM section, the general trend that NHC-based catalysts are more efficient than their phosphine-based analogues is readily apparent, although exceptions were discovered. Moreover, it is important to note that there is no single best or most efficient catalyst for all RCM reactions. For simple substrates (eq A1.1), catalyst activity seems to be the most important factor, but for more challenging reactions stability becomes increasingly important. This was nicely illustrated by the very different performances of **H_2IDIPP–P** and **IMes–P**. Whereas **H_2IDIPP–P** (active, less stable) can catalyze the RCM of **A1.8** faster than any other

catalyst in this assay, it is not stable enough to achieve complete conversion for the synthesis of **A1.11** and is inefficient for the preparation of tetrasubstituted double bonds. The activity profile for **IMes–P** is very different since it is a considerably more stable but less active catalyst. It is less efficient in the RCM of **A1.8** than the phosphine-based **PCy_3–O** and less efficient than **H_2IMes–P** in the RCM to form **A1.11**. Its increased stability, however, renders it the most efficient catalyst from our selection in the RCM to form tetrasubstituted olefins.

Cross Metathesis

Olefin cross metathesis (CM) is an intermolecular subset of olefin metathesis. In CM the identity of the olefins plays a major role in product selectivity. The two main issues in product selectivity are stereoselectivity (*E* versus *Z* olefin), and chemoselectivity, which determines the ratio of heterocoupled to homocoupled product. A nonchemoselective catalyst will afford the desired product in a statistically determined maximum of 50% yield if the starting olefins are used in a 1:1 ratio.[17] These features make CM reactions ideal for assessing catalyst behavior, with a particular emphasis on selectivity.

CM of Allylbenzene and Cis-1,4-Diacetoxy-2-Butene

Allylbenzene (**A1.14**) and 1,4-diacetoxy-2-butene (**A1.15**) show similar behavior in metathesis reactions. Hence, to increase the statistical yield of the desired heterocoupled product **A1.16**, 2 equiv of **A1.15** (corresponding to 4 equiv of allylacetate) are used (eq A1.4). The reaction was chosen as the first CM screen because of its reproducibility and the important information it provides about *E*/*Z* selectivity. Although only the desired heterocoupled product is shown in eq A1.4, all six reaction components (*E*/*Z* heterocoupled product **A1.16**, *E*/*Z* 1,4-diacetoxy-2-butene (**A1.15**), *E*/*Z* homocoupled allylbenzene) are observed and can be readily monitored by GC during the course of the reaction. The conversions to heterocoupled product versus time using catalysts **A1.1**–**A1.7** are plotted in Figures A1.6 and A1.7. There is a general distinction between the activity of the first- and second-generation catalysts, the latter being significantly more active, as illustrated by the decreased reaction times and higher total

conversions. Overall, the reactivity trends for CM were found to be similar to those observed for RCM. The plots shown in Figures A1.8 and A1.9 track the *E*/*Z* ratio of product as a function of conversion to **A1.16**. From this analysis, a significant difference in the *E*/*Z* profile between first- and second-generation catalysts is apparent. For the first-generation catalysts the *E*/*Z* ratio stays relatively constant (~5). In contrast, the NHC-based catalysts produce a product with lower *E*/*Z* ratios (~3) at low conversion, but as the conversion increases above 60% the product *E*/*Z* ratios increase dramatically. Presumably, the difference between the two catalyst classes can be rationalized on the basis of the greater ability of second-generation catalysts to promote secondary metathesis, isomerizing the product to the thermodynamically favored *E* isomer (ratio ~10). At low conversion the *E*/*Z* ratio appears to be controlled, at least to some extent, by the inherent diastereoselectivity of the catalyst. The similarity between the *E*/*Z* profiles of the catalysts in Figure A1.9 is striking and suggests that *E*/*Z* selectivity at high conversion is governed by thermodynamic factors much more than it is by the inherent properties of the catalysts. The development of new catalysts that can kinetically control *E*/*Z* selectivity is therefore a challenging, yet important, task for future research.

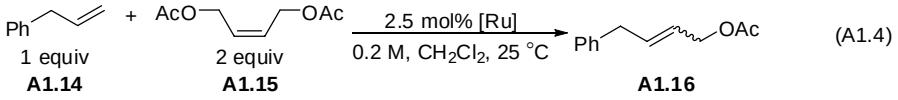

(A1.4)

CM of Methyl Acrylate and 5-Hexenyl Acetate

In contrast to the CM reaction presented above, different olefin metathesis catalysts exhibit different behavior with respect to the two olefins in this CM reaction. While 5-hexenyl acetate (**A1.17**) has a similar reactivity to allylbenzene, methyl acrylate (**A1.18**) only dimerizes slowly under metathesis reaction conditions.[18] This difference in reactivity allows for chemoselective CM, in which the product yield is not statistical. Instead, the reaction is driven to high conversion by the reactivity difference between the two olefins. Methyl acrylate (**A1.18**) is a challenging substrate in olefin metathesis, thereby rendering this CM (eq A1.5) a more demanding reaction than that discussed above. However, this reaction is a better indicator for

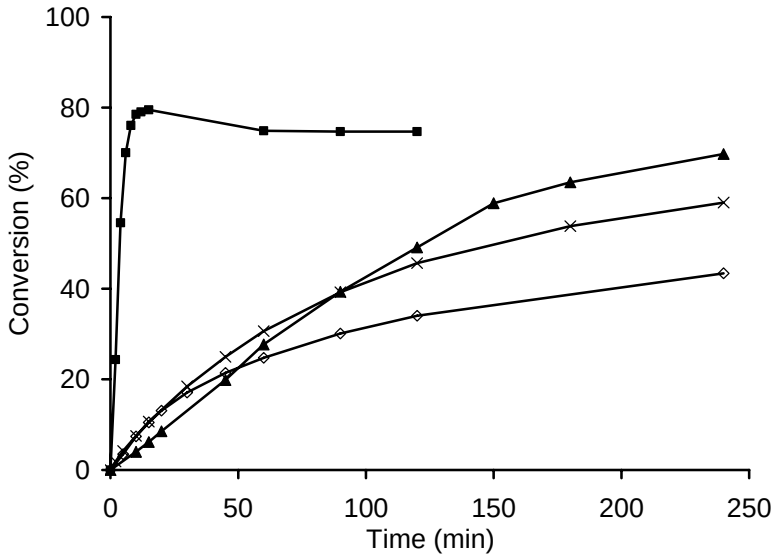

Figure A1.6. Conversion to heterocoupled product **A1.16** using **PCy_3–P**(×), **PCy_3–O**(◇), **H_2IMes–P**(■), and **IMes–P**(▲).

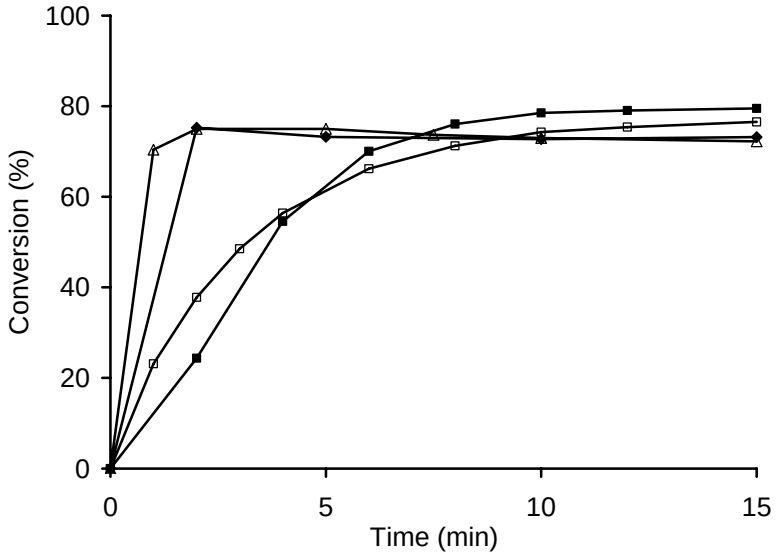

Figure A1.7. Conversion to heterocoupled product **A1.16** using **H_2IMes–P**(■), **H_2IMes–O**(△), **H_2IDIPP–P**(◆), and **H_2IMes–py**(□).

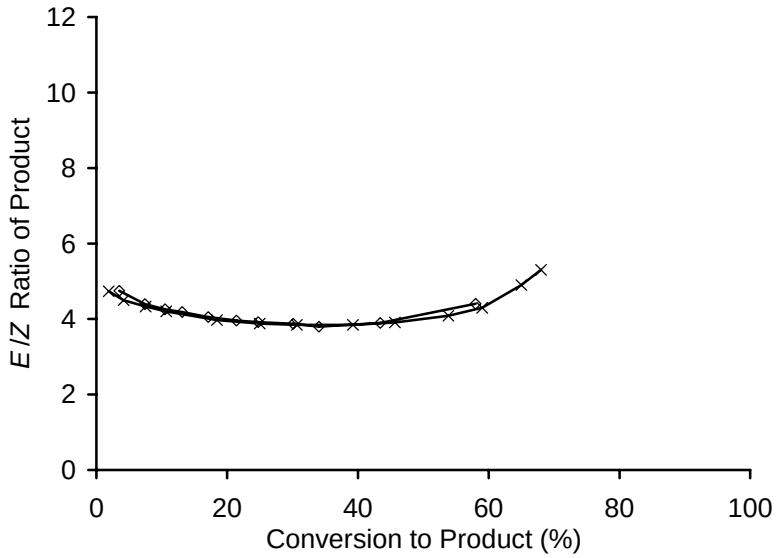

Figure A1.8. *E*/*Z*-selectivity vs conversion, first generation (eq A1.4) **PCy$_3$–P**(×) and **PCy$_3$–O**(◇).

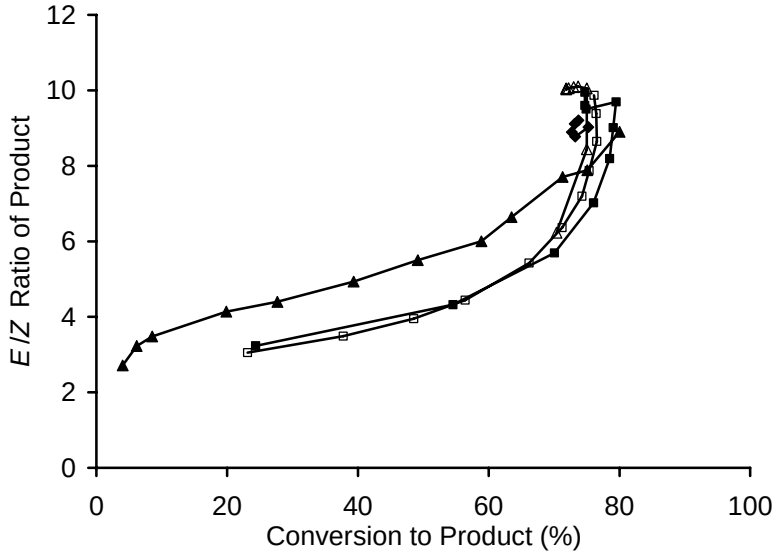

Figure A1.9. *E*/*Z*-selectivity of **A1.16** vs conversion to **A1.16**, second generation (eq A1.4) **H$_2$IMes–P**(■), **H$_2$IMes–O**(△), **IMes–P**(▲), **H$_2$IDIPP–P**(◆), and **H$_2$IMes–py**(□).

catalyst reactivity toward a variety of electron-deficient olefins. The only CM product observed is the *E* isomer, presumably due to the strong preference to form the *E*-configured unsaturated ester. As shown in Figure A1.10, first-generation catalysts do not catalyze this reaction to a synthetically useful extent: no more than 10% of product can be observed. Instead, 80% of

A1.17 is homocoupled after 6 h, indicating that while phosphine-based catalysts do efficiently catalyze the CM of terminal, unhindered olefins, they do not react with electron-poor, conjugated olefins.[19] The higher conversion to product exhibited by NHC-based catalysts is illustrated in Figure A1.10. The increased reactivity of NHC-based catalysts toward functionalized olefins relative to phosphine-based catalysts is evident. It is this increased reactivity toward olefins with different properties that tremendously influenced the development of chemoselective CM reactions and rendered CM a useful, predictable, and reliable synthetic method.[20] With the NHC-based catalysts, the same activity and stability trends already seen in RCM were observed. This is well illustrated by the greater activity of **H_2IMes–P** than **IMes–P**, and the low stability of **H_2IMes–py**.

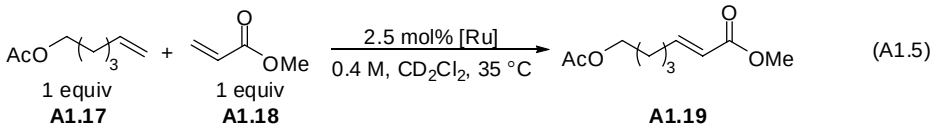

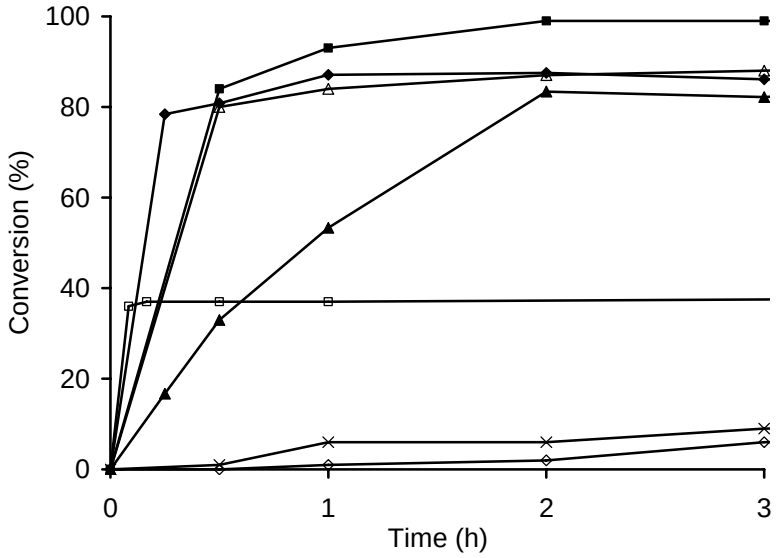

Figure A1.10. Conversion to heterocoupled product **A1.19** **PCy_3–P**(×), **PCy_3–O**(◇), **H_2IMes–P**(■), **H_2IMes–O**(△), **IMes–P**(▲), **H_2IDIPP–P**(◆), and **H_2IMes–py**(□).

Ring-opening metathesis polymerization

ROMP of cyclic olefins is a common application for olefin metathesis (eq A1.6).[21] Frequently used monomers for ROMP include norbornene and norbornene derivatives. These, however, are highly strained systems that polymerize very quickly making accurate monitoring of the reaction progress difficult. The ROMP of 1,5-cyclooctadiene (**A1.20**), on the other hand, can be conveniently followed by NMR spectroscopy at a monomer to catalyst ratio of 1000:1. In this reaction a single starting material cleanly converts to one product without the formation of any byproducts, facilitating analysis. Furthermore, in contrast to all other standard reactions of this assay, none of the less stable ruthenium methylidene complex is formed at any time during the reaction.[22] This might be one of the reasons this reaction can be efficiently carried out at low catalyst loadings. The polyalkenamer formed contains both *E* and *Z* olefins, for which the ratio has not been quantified but does change during the course of the reaction, indicating secondary metathesis is in operation on existing polymer chains.[23] The conversions to product over time are represented in Figure A1.11. The efficiency of **H_2IMes–py** is remarkable, affording complete conversion before the first measurement could be taken after 30 s. Unlike most of the other presented reactions, stability seems to play only a marginal role in this transformation: catalyst activity has the larger contribution to catalyst efficiency. Although reactive, first-generation catalysts are dramatically less active in this transformation. For many catalysts an initial induction period was observed. After this induction period, the reaction follows pseudo-first-order kinetics. Rate constants can be obtained from these data, allowing for quantitative comparison of the reaction rates (see Experimental section).

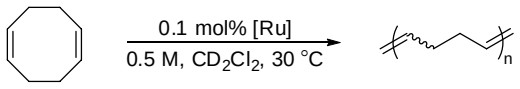

(A1.6)

A1.20 **poly(A1.20)**

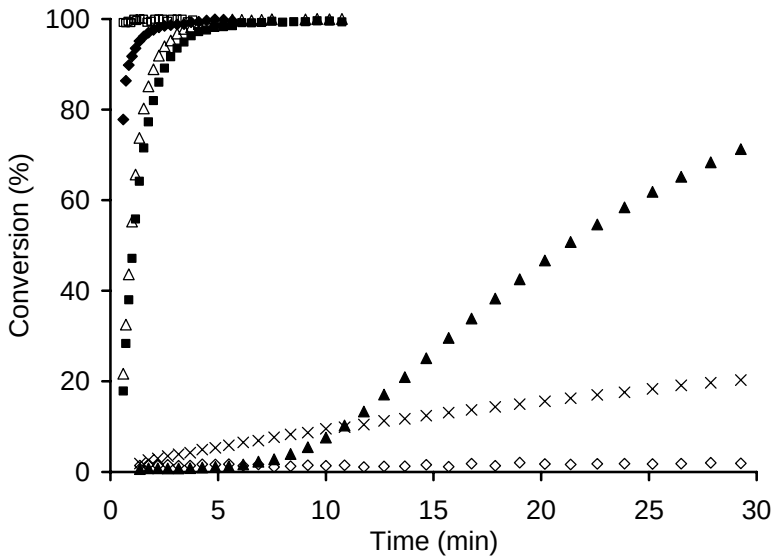

Figure A1.11. Conversion to polymer product Poly(**A1.20**) **PCy_3–P**(×), **PCy_3–O**(◇), **H_2IMes–P**(■), **H_2IMes–O**(△), **IMes–P**(▲), **H_2IDIPP–P**(◆), and **H_2IMes–py**(□).

Conclusions

In conclusion, we have established a set of standardized reactions to characterize olefin metathesis catalysts. We have compared seven of the most common ruthenium-based olefin metathesis catalysts and described them in terms of efficiency, characterized by selectivity, activity, and stability. During this comparison it became evident that there is no single best catalyst available, and it is unlikely that such a catalyst will be developed. Instead, the relative efficiencies of a set of catalysts can only be compared within a single reaction or reaction class (e.g., RCM). Our findings include the importance of highly active catalysts for easy metathesis reactions such as ROMP and RCM of unhindered olefins, the increasing importance of stability with more challenging reactions such as RCM to form tetrasubstituted double bonds, the increased reactivity of NHC-based catalysts toward functionalized olefins, and the current unavailability of inherently *Z*- or *E*-selective catalysts. Additionally, we observed intriguing behavior in the RCM of **A1.8** with **PCy_3–P** for the first time, despite the fact that this catalyst has been known and widely used for over a decade. The important quantitative data obtained from a handful of simple experiments should serve as a foundation for catalyst analysis and further design. We believe that a general set of standard reaction screens will not only be a great

service to research groups interested in olefin metathesis, but hopefully, also serve as an example for the development of similar standards in other areas of catalysis.

Experimental Section

General Considerations. Unless otherwise indicated, all compounds were purchased from Aldrich or Fisher. Allylbenzene, tridecane, and *cis*-1,4-diacetoxy-2-butene were distilled from anhydrous potassium carbonate prior to use. (Compounds can also be distilled and stored in degassed Schlenk flasks for extended periods of time.) Anhydrous dichloromethane (purchased from Fisher) was obtained via elution through a solvent column drying system.[24] 5-Hexenyl acetate (Aldrich) was distilled and stored in a sealed vial under Ar. Methyl acrylate (Aldrich, 99%) was used as received. Anthracene (Aldrich) was used as received. CD_2Cl_2 was purchased from Cambridge Isotope Laboratories, distilled from CaH_2 into a Schlenk tube, and freeze/pump/thawed 3 times. Catalysts were received as gifts from Materia, Inc. *cis*,*cis*-1,5-Cyclooctadiene (Aldrich) was distilled immediately prior the polymerization reaction, as aged *cis*,*cis*-1,5-cyclooctadiene afforded inferior results. Gas chromatography data was obtained using an Agilent 6850 FID gas chromatograph equipped with a DB-Wax Polyethylene Glycol capillary column (J&W Scientific).

Stock Solution Preparation. A single stock solution can be prepared that contains enough catalyst for all three RCM reactions as well as the ROMP reaction. Inside a glovebox, a volumetric flask is charged with catalyst (0.016 mmol) and CD_2Cl_2 added to prepare 1.0 mL of stock solution (0.016 M).

RCM of Diethyldiallyl malonate (A1.8). An NMR tube with a screw-cap septum top was charged inside a glovebox with catalyst stock solution (0.016 M, 50 μL, 0.80 μmol, 1.0 mol%) and CD_2Cl_2 (0.75 mL). The sample was equilibrated at 30 º C in the NMR probe before **A1.8** (19.3 μL, 19.2 mg, 0.080 mmol, 0.1 M) was added via syringe. Data points were collected over an appropriate period of time using the Varian array function. The conversion to **A1.9** was

determined by comparing the ratio of the integrals of the methylene protons in the starting material, δ 2.61 (dt), with those in the product, δ 2.98 (s).

RCM of Diethylallylmethallyl malonate (A1.10). An NMR tube with a screw-cap septum top was charged inside a glovebox with catalyst stock solution (0.016 M, 50 μL, 0.80 μmol, 1.0 mol%) and CD_2Cl_2 (0.75 mL). The sample was equilibrated at 30 º C in the NMR probe before **A1.10** (20.5 μL, 20.4 mg, 0.080 mmol, 0.1 M) was added via syringe. Data points were collected over an appropriate period of time using the Varian array function. The conversion to **A1.11** was determined by comparing the ratio of the integrals of the methylene protons in the starting material, δ 2.67 (s), 2.64 (dt), with those in the product, δ 2.93 (s), 2.88 (m).

RCM of Diethyldimethallyl malonate (A1.12). An NMR tube with a screw-cap septum top was charged inside a glovebox with catalyst stock solution (0.016 M, 250 μL, 4.0 μmol, 5.0 mol%) and CD_2Cl_2 (0.55 mL). Olefin **A1.12** (21.6 μL, 21.5 mg, 0.080 mmol, 0.1 M) was added via syringe and the sample placed in an oil bath regulated at 30 ºC. A ^{1}H NMR spectrum was taken after 4 d. The conversion to **A1.13** was determined by comparing the ratio of the integrals of the methylene protons in the starting material, δ 2.71 (s), with those in the product, δ 2.89 (s).

Table A1.2. k_{obs} Values (**A1.8** to **A1.9**)

Catalyst	k_{obs} (s^{-1})
1	--
2	0.0016[a]
3	0.0022
4	0.0030
5	0.00075
6	>0.04
7	>0.0041[b]

[a] After induction period, measured from 25–90%.
[b] First 50% conversion used.

Table A1.3. k_{obs} Values (**A1.10** to **A1.11**)

Catalyst	k_{obs} (s^{-1})
1	--
2	0.00011[a]
3	0.0012
4	0.0012
5	0.00038
6	>0.01
7	>0.0018[b]

[a] After induction period, measured from 25–90%.
[b] First 25% conversion used.

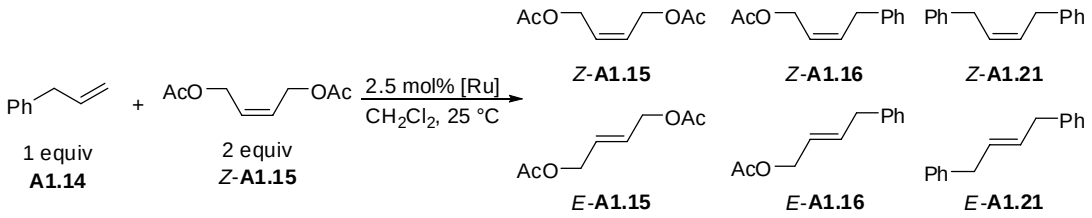

Cross metathesis of allylbenzene with *cis*-1,4-diacetoxy-2-butene. Allylbenzene (1.00 mL, 7.55 mmol) and tridecane (0.920 mL, 3.77 mmol) were combined in a flame-dried, 1-dram vial under an atmosphere of argon. The mixture was stirred before taking a t_o timepoint. Reactions were run with 51 μL of this solution in lieu of adding the allylbenzene and tridecane separately. To a flame-dried 1-dram vial, 5.0 μmol of catalyst was added. The vial was purged with argon (~5 min), and then 1.0 mL of anhydrous dichloromethane was added. *cis*-1,4-Diacetoxy-2-butene (64 μL, 0.40 mmol) and the allylbenzene/tridecane mixture (51 μL; 0.20 mmol 14 + 0.10 mmol tridecane) were then added via syringe. The reaction was allowed to stir at 23 ºC. Aliquots were taken at the specified time periods. Samples for GC analysis were obtained by adding ca. 30-μL reaction aliquot to 500 μL of a 3M solution of ethyl vinyl ether in dichloromethane. The sample was shaken, allowed to stand for 5 min, and then analyzed via GC. All reactions were performed in duplicate to confirm reproducibility.

Cross metathesis of methyl acrylate and 5-hexenyl acetate. 5-Hexenyl acetate (88 mg, 100 μL, 0.62 mmol) and methyl acrylate (54 mg, 56 μL, 0.62 mmol) were added to a solution of anthracene (15–20 mg) in 1.55 mL CD_2Cl_2 in a 10 mL round-bottomed flask under argon topped with a reflux condenser. An aliquot of 100 μL was removed from the solution and was diluted with CD_2Cl_2 in an NMR tube (this is the t = 0 point). The reaction solution was heated to 35 °C and catalyst (0.015 mmol, 2.5 mol % after removal of 100 μL aliquot) was added in one portion. Aliquots (50–100 μL) were removed from the reaction solution at the desired times, diluted with CD_2Cl_2 in an NMR tube, and cooled to –78 °C until the NMR spectrum was taken. Attempts to perform this reaction in an NMR tube or in a sealed flask resulted in incomplete conversions due to ethylene build-up. All conversions were determined relative to the anthracene internal standard. The anthracene multiplet at 7.48 ppm was given an integration of 1.00 in the spectrum at each time point. The multiplet at 4.98 ppm (2 H; $C=CH_2$ of 5-hexenyl acetate) and the doublet of doublets at 6.37 ppm (1H; *J* = 17.3, 1.7 Hz; *cis*-C=CHH of methyl acrylate) were used as peaks to monitor the disappearance of the starting materials. Product formation was determined two ways: (1) the disappearance of methyl acrylate; (2) the integration of the doublet of triplets at 6.93 ppm (1 H; *J* = 15.7, 7.2 Hz; C=CHR) divided by the sum of the integrations of the peaks at 6.37 ppm and 6.93 ppm. Typically the difference between these two methods was no greater than 5%. *Characterization of* ***A1.19*****.** ^{1}H NMR (300 MHz, $CDCl_3$, δ): 6.93 (dt, *J* = 15.7, 7.2 Hz, 1 H), 5.81 (dt, *J* = 15.7, 1.4 Hz, 1 H), 4.04 (t, *J* = 6.3 Hz, 2 H), 3.70 (s, 3 H), 2.22 (dq, *J* = 7.2, 1.4 Hz, 2 H), 2.02 (s, 3 H), 1.59–1.66 (m, 2 H), 1.48–1.56 (m, 2 H). ^{13}C NMR (75 MHz, $CDCl_3$, δ): 171.3, 167.2, 148.9, 121.5, 64.2, 51.6, 31.8, 28.2, 24.6, 21.1.

ROMP of 1,5-cyclooctadiene (A1.20). An NMR tube with a screw-cap septum top was charged inside a glovebox with catalyst stock solution (0.016 M, 25 μL, 0.40 μmol, 0.1 mol%) and CD_2Cl_2 (0.775 mL). The sample was equilibrated at 30 º C in the NMR probe before **A1.20** (49.1 μL, 43.3 mg, 0.40 mmol, 0.5 M) was added via syringe. Data points were collected over an appropriate period of time using the Varian array function. The conversion to poly(**A1.20**) was determined by

comparing the ratio of the integrals of the methylene protons in the starting material, δ 2.36 (m), with those in the product, δ 2.09 (br m), 2.04 (br m).

Table A1.4. k_{obs} Values Where Appropriate (**A1.20** to poly(**A1.20**))

Catalyst	k_{obs} (s^{-1})
1	--
2	--
3	0.016
4	0.020
5	0.0012
6	--
7	--[1]

[1] > 95% conversion in < 36 s

References and Notes

[1] Grubbs, R. H., Ed. *Handbook of Metathesis*; Wiley-VCH: Weinheim, Germany, 2003.

[2] Wakamatsu, H.; Blechert, S. *Angew. Chem., Int. Ed.* **2002**, *41*, 2403–2405.

[3] Hong, S. H.; Grubbs, R. H. *J. Am. Chem. Soc.* **2006,** *128,* 3508–3509.

[4] Catalysts nomenclature denotes the nondissociating ligand as well as the dissociating ligand in the name, where **P** stands for PCy_3, **O** stands for the chelating ether ligand, and **py** stands for 3-bromopyridine (e.g., **H_2IMes–P**, denotes the nondissociating **H_2IMes** and **P** the dissociating PCy_3).

[5] Molybdenum-based olefin metathesis catalysts were not compatible with the experimental protocols used due to their instability toward air and moisture. For details, see the Experimental Section. For lead articles for molybdenum catalysts, see (a) Schrock, R. R.; Murdzek, J. S.; Bazan, G. C.; Robbins, J.; Dimare, M.; O'Regan, M. *J. Am. Chem. Soc.* **1990**, *112*, 3875–3886. (b) Schrock, R. R. *Acc. Chem. Res.* **1990**, *23*,158–165.

[6] Schwab, P.; Grubbs, R. H.; Ziller, J. W. *J. Am. Chem. Soc.* **1996,** *118,* 100–110.

[7] (a) Harrity, J. P. A.; La, D. S.; Cefalo, D. R.; Visser, M. S.; Hoveyda, A. H. *J. Am. Chem. Soc.* **1998,** *120,* 2343–2351. (b) Kingsbury, J. S.; Harrity, J. P. A.; Bonitatebus, P. J.; Hoveyda, A. H. *J. Am. Chem. Soc.* **1999,** *121,* 791–799.

[8] Scholl, M.; Ding, S.; Lee, C. W.; Grubbs, R. H. *Org. Lett.* **1999,** *1,* 953–956. Molybdenum-based catalysts are efficient for this transformation, see: Kirkland, T. A.; Grubbs, R. H. *J. Org. Chem.* **1997**, *62*, 7310–7318.

[9] (a) Garber, S. B.; Kingsbury, J. S.; Gray, B. L.; Hoveyda, A. H. *J. Am. Chem. Soc.* **2000,** *122,* 8168–8179. (b) Gessler, S.; Randl, S.; Blechert, S. *Tetrahedron Lett.* **2000,** *41,* 9973–9976.

[10] (a) Scholl, M.; Trnka, T. M.; Morgan, J. P.; Grubbs, R. H. *Tetrahedron Lett.* **1999,** *40,* 2247–2250. (b) Huang, J.; Stevens, E. D.; Nolan, S. P.; Petersen, J. L. *J. Am. Chem. Soc.* **1999,** *121,* 2674–2678.

[11] Dinger, M. B.; Mol, J. C. *Adv. Synth. Catal.* **2002,** *344,* 671–677.

[12] (a) Love, J. A.; Morgan, J. P.; Trnka, T. M.; Grubbs, R. H. *Angew. Chem. Int. Ed.* **2002,** *41,* 4035–4037. (b) Sanford, M. S.; Love, J. A.; Grubbs, R. H. *Organometallics* **2001,** *20,* 5314–5318.

[13] Grubbs, R. H., Ed. *Handbook of Metathesis*; Wiley-VCH: Weinheim, Germany, 2003; Vol. 2.

[14] (a) Trnka, T. M.; Grubbs, R. H. *Acc. Chem. Res.* **2001,** *34,* 18–29. (b) Trnka, T. M.; Morgan, J. P.; Sanford, M. S.; Wilhelm, T. E.; Scholl, M.; Choi, T.-L.; Ding, S.; Day, M. W.; Grubbs, R. H. *J. Am. Chem. Soc.* **2003,** *125,* 2546–2558. (c) Love, J. A.; Sanford, M. S.; Day, M. W.; Grubbs, R. H. *J. Am. Chem. Soc.* **2003,** *125,* 10103–10109. (d) Yun, J.; Marinez, E. R.; Grubbs, R. H. *Organometallics* **2004,** *23,* 4172–4173. (e) Ung, T.; Hejl, A.; Grubbs, R. H.; Schrodi, Y. *Organometallics* **2004,** *23,* 5399–5401. (f) Despagnet-Ayoub, E.; Grubbs, R. H. *Organometallics* **2005,** *24,* 338–340.

[15] (a) Van Veldhuizen, J. J.; Gillingham, D. G.; Garber, S. B.; Kataoka, O.; Hoveyda, A. H. *J. Am. Chem. Soc.* **2003,** *125,* 12502–12508. (b) Michrowska, A.; Bujok, R.; Harutyunyan, S.; Sashuk, V.; Dolgonos, G.; Grela, K. *J. Am. Chem. Soc.* **2004,** *126,* 9318–9325. (c) Slugovc, C.; Perner, B.; Stelzer, F.; Mereiter, K. *Organometallics* **2004,** *23,* 3622–3626. (d) Romero, P. E.; Piers, W. E.; McDonald, R. *Angew. Chem. Int. Ed.* **2004,** *43,* 6161–6165. (e) Conrad, J. C.; Parnas, H. H.; Snelgrove, J. L.; Fogg, D. E. *J. Am. Chem. Soc.* **2005,** *127,* 11882–11883.

[16] Courchay, F. C.; Sworen, J. C.; Wagener, K. B. *Macromolecules* **2003,** *36,* 8231–8239.

[17] Chatterjee, A. K.; Choi, T.-L.; Sanders, D. P.; Grubbs, R. H. *J. Am. Chem. Soc.* **2003**, *125*, 11360–11370.

[18] For references pertaining to the CM of α,β-unsaturated compounds, see: (a) Chatterjee, A. K.; Morgan, J. P.; Scholl, M.; Grubbs, R. H. *J. Am. Chem. Soc.* **2000**, *122*, 3783–3784; (b) Choi, T.-L. Lee, C. W.; Chatterjee, A. K.; Grubbs, R. H. *J. Am. Chem. Soc.* **2001**, *123*, 10417–10418; (c) Choi, T.-L.; Chatterjee, A. K.; Grubbs, R. H. *Angew. Chem., Int. Ed.* **2001**, *40*, 1277–1279; (d) Cossy, J.; BouzBouz, S.; Hoveyda, A. H. *J. Organomet. Chem.* **2001**, *624*, 327–332; Chatterjee, A. K.; Toste, F. D.; Choi, T.-L.; Grubbs, R. H. *Adv. Synth. Catal.* **2002**, *344*, 634–637.

[19] Blackwell, H. E.; O'Leary, D. J.; Chatterjee, A. K.; Washenfelder, R. A.; Bussmann, D. A.; Grubbs, R. H. *J. Am. Chem. Soc.* **2000**, *122*, 58–71.

[20] For reviews, see: (a) Chatterjee, A. K. Olefin Cross-Metathesis. In *Handbook of Metathesis*, Grubbs, R. H., Ed.; Wiley-VCH: Weinheim, Germany, 2002; Vol. 2, pp 246–295. (b) Wenzel, A. G.; Chatterjee, A. K.; Grubbs, R. H. In *Comprehensive Organometallic Chemistry III*; Crabtree, R.; Mingos, M., Eds.; Elsevier: Oxford, 2007; Chapter 11.08.

[21] (a) Grubbs, R. H., Ed. *Handbook of Metathesis*; Wiley-VCH: Weinheim, Germany, 2003; Vol. 3. (b) Slugovc, C. *Macromol. Rapid Commun.* **2004,** *25,* 1283–1297.

[22] Ulman, M.; Grubbs, R. H. *J. Org. Chem.* **1999**, *54*, 7202–7207.

[23] Bielawski, C. W.; Grubbs, R. H. *Angew. Chem. Int. Ed.* **2000,** *39,* 2903–2906.

[24] Pangborn, A. B.; Giardello, M. A.; Grubbs, R. H.; Rosen, R. K.; Timmers, F. J. *Organometallics* **1996**, *15*, 1518–1520.